Macromolecules

Article

pubs.acs.org/Macromolecules

Nucleosome-like Structure from Dendrimer-Induced DNA Compaction

Chun-Jen Su,*[,†] Chun-Yu Chen,[†] Ming-Champ Lin,[‡] Hsin-Lung Chen,*[,‡] Hiroki Iwase,[§] Satoshi Koizumi,[§] and Takeji Hashimoto[‡,§,⊥]

[†]National Synchrotron Radiation Research Center, Hsin-Chu 300, Taiwan

[‡]Department of Chemical Engineering and Frontier Research Center on Fundamental and Applied Sciences of Matters, National Tsing Hua University, Hsin-Chu 30013, Taiwan

[§]Advanced Science Research Center, Japan Atomic Energy Agency, Naka-gun, Ibaraki Pref. 319-1195, Japan

ABSTRACT: Genomic DNA in eukaryotes wraps around histone proteins to package into the limited space of cell nucleus. Since the precise structure of chromatin is not known in detail, attempts have been made to understand DNA–histone interaction and the associated self-organization behavior using synthetic model systems. Using small-angle X-ray and neutron scattering, here we show that the electrostatic attraction between DNA and polyamidoamine (PAMAM) dendrimer of generation nine (G9) led to the formation of beads-on-string structure, where DNA wrapped around the dendrimer tightly to yield the "chromatin-like fiber" composing of the interconnected "nucleosome-like particles". A "stiff chromatin-like fiber model" and a "wormlike chromatin-like fiber model" were introduced to obtain the theoretical scattering patterns closely resembling the experimentally observed ones, from which the pitch length (P) of the DNA superhelix wrapping around the dendrimer and the interparticle distance (d) of the nucleosome-like particles were deduced. Governed by the balance between the electrostatic interaction energy and DNA bending energy, P and d were found to decrease and increase with increasing charge density of dendrimer, respectively. The chromatin-like fibers formed at lower dendrimer charge densities exhibited certain conformational flexibility characterized by the orientation fluctuations of the nucleosome-like particles. The fiber however stiffened when the dendrimer charge density was increased to the extent that all the primary amine groups at the surface of the dendrimer were protonated. The present study revealed not only the accessibility of the beads-on-string structure by a potential model system for histone protein but also the effect of macrocation charge density on the DNA wrapping mode and the conformational feature associated with the chromatin-like fiber formed by the dendriplex.

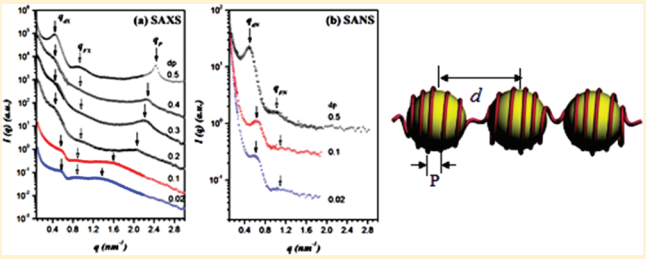

INTRODUCTION

Compaction of DNA is important because DNA is stored and functions in a compact form of various densities in living organisms. In eukaryotic cells, over a meter of DNA is packaged into condensed chromatin to fit within the limited volume of the nucleus.[1,2] The formation of chromatin involves local wrapping of ca. 147 bps of DNA around an octamer of histone protein to form nucleosome particles which are interconnected by the linker DNA. Through the mediation of H1 histone, the nucleosome array successively folds into compact filament with well-defined higher-order structure.[3]

Since nucleosome is the principal packaging element of DNA within the nucleus and the precise structure of chromatin fiber is not known in detail, theoretical and experimental attempts have been made to understand the interaction between DNA and histone and the associated self-organization behavior using synthetic model systems whose properties (e.g., charge density, charge ratio, molecular geometry, etc.) can be systematically varied for facilitating the resolution of structure formation mechanism and dynamics. Theoretically, DNA and histone have been modeled by semiflexible polyelectrolyte and spherical macrocation, respectively.[4] Various simulation studies have consistently predicted that the electrostatic attraction leads more or less to tight wrapping of the semiflexible chain around oppositely charged spheres, yielding the "beads-on-string" structure.[5−7] Salt concentration was found to play a significant role controlling the wrapping mode.[6,7] Unlike the theoretical works, the relevant experimental study is limited by the difficulty of identifying a convenient model system for histone. Recently, Zinchenko et al. used positively charged silica nanoparticles as the artificial model for histone and investigated their interaction with DNA.[8,9] Both particle size and salt concentration were found to have a profound influence on the wrapping mode of DNA around the particles.

Dendrimers are a class of hyperbranched macromolecule composing of layers of monomer units irradiating from a central core; each complete grafting cycle is called a "generation" (denoted by Gn with n being the generation

Received: February 17, 2012
Revised: May 8, 2012
Published: June 4, 2012

number).[10,11] Dendrimers are monodisperse and possess specific size, shape characteristics, and tunable surface functionality. Polyamidoamine (PAMAM) is the most common type of dendrimer with well-defined number of functional amine groups at the surface and the interior. These amine groups can be protonated to controlled level in acidic aqueous environment to generate macrocations capable of forming electrostatic complex with DNA (called "dendriplex").[12]

PAMAM dendrimers with high generation numbers are spherical in shape and may thus be useful model system for histone protein considering their geometric similarity and tunable charge density of the dendrimer.[13] Nevertheless, previous studies of dendriplexes were predominantly motivated by the potential application of the complexes in nonviral gene delivery,[14] while little attention has been directed to exploring the suitability of the dendriplexes to structurally mimic nucleosome particle or chromatin fiber. A prerequisite of a dendrimer to act as an artificial model of histone is the induction of DNA to wrap around it to form the "nucleosome-like" particle. The occurrence of such a beads-on-string structure should be largely governed by the balance between the electrostatic attraction and the bending energy of DNA.[6,7,15] Tight wrapping around the macrocation enhances charge matching but increases DNA bending free energy; therefore, beads-on-string configuration may not be accessible for the complexes with low-generation dendrimers because of high bending energy cost associated with large surface curvature. Alternatively, the complexation induces aggregation of the locally extended DNA chains bridged by the dendrimer to yield the "columnar mesophases".[16−18]

Beads-on-string structure should become accessible at high dendrimer generations;[19,20] however, the nucleosome-like structure in such dendriplex systems has not been studied systematically. The fundamental problems concerning the condition of the occurrence of beads-on-string structure, DNA wrapping mode, and the global organization of the nucleosome-like dendriplex particles remain to be addressed.

In this study, we demonstrate the full access of beads-on-string structure in the dendriplexes with PAMAM G9 dendrimer. Synchrotron small-angle X-ray scattering (SAXS) and small-angle neutron scattering (SANS) were employed to reveal the structural details ranging from the internal structure of the nucleosome-like particles formed to the organization of these particles on a more global length scale as a function of the charge density of G9 dendrimer. It will be shown that DNA was able to wrap around G9 dendrimer tightly even at very low charge density, and the pitch length of the DNA superhelix depended on the charge density. Moreover, two distinct types of conformational flexibility of the chromatin-like fiber composing of the interconnected nucleosome-like dendriplex particles will be identified from the analysis of the scattering patterns.

EXPERIMENTAL SECTION

1. Materials. Linear calf thymus DNA was purchased from ICN and used without further purification. Its molecular weight was ca. 9.2 kbps. Ethylenediamine (EDA) core PAMAM G9 dendrimer was obtained from Dendritic Nanotechnologies, Inc., as methanol solutions. After thorough drying, the solids were weighed and then redissolved in D_2O to produce a stock solution of 0.1% (w/w). The solutions were stored at 4 °C until use.

2. Complex Preparation. To complex with the polyanionic DNA, the amine groups in PAMAM dendrimer were first protonated by adding prescribed amount of 0.1 N HCl solution. The primary amine groups at the outer surface of the dendrimer tended to be protonated first because their basicity ($pK_a \cong 9.0$) is larger than that of the interior tertiary amines ($pK_a \cong 5.8$).[21] Therefore, the PAMAM G9 dendrimers with different degrees of protonation (dp) were prepared by controlling the pH of the solution. The solution of the protonated dendrimer was then mixed with the aqueous solution containing prescribed amount of DNA to obtain the complex. The concentration of DNA aqueous solution was 2 mg/mL. The complexaton was usually manifested by visually observable precipitation.

3. Small-Angle X-ray Scattering (SAXS) Measurements. The structures of the dendriplexes were probed by SAXS at room temperature. The aqueous suspensions of the complexes were directly introduced into the sample cell comprising of two kapton windows. The SAXS experiments were performed at the Endstation BL23A1 of the National Synchrotron Radiation Research Center (NSRRC), Taiwan. The energy of X-ray source and sample-to-detector distance were 14 keV and 2259 mm, respectively. The scattering signals were collected by MarCCD detector of 512 × 512 pixel resolution. The scattering intensity profile was output as the plot of the scattering intensity $I(q)$ vs the scattering vector, $q = (4\pi/\lambda)\sin(\theta/2)$ (θ = scattering angle), after corrections for sample transmission, empty cell transmission, empty cell scattering, and the detector sensitivity.

4. Small-Angle Neutron Scattering (SANS) Measurements. SANS experiments were conducted with the SANS-J spectrometer installed at JRR-3 research reactor at JAEA, Tokai, Japan. The experiments were conducted with the incident neutron wavelength of 0.65 nm and the sample-to-detector distances of 2.5 and 10.2 m to access the q range of 0.04−1.0 nm^{-1}. The high-q range was further extended to 2.8 nm^{-1} with the change of neutron wavelength to 0.43 nm and the tilted angle of the flight tube to 4.1°.

RESULTS AND DISCUSSION

1. Features of Scattering Profiles. Here we use SAXS and SANS to probe the structures of the dendriplexes in D_2O. The scattering intensity of the complex can be factorized into three partial structure factors, viz.[16]

$$I(q) = \Delta\rho_{DNA}{}^2 S_{DD}(q) + 2\Delta\rho_{DNA}\Delta\rho_{den} S_{Dd}(q) + \Delta\rho_{den}{}^2 S_{dd}(q) \quad (1)$$

where $S_{DD}(q)$, $S_{dd}(q)$, and $S_{Dd}(q)$ are the partial structure factors associated with DNA−DNA, dendrimer−dendrimer, and DNA−dendrimer correlations, respectively; $\Delta\rho_{DNA}$ and $\Delta\rho_{den}$ are the scattering length density (SLD) contrast of DNA and dendrimer relative to D_2O, respectively. The calculated X-ray SLD of DNA, dendrimer, and D_2O is 15.0×10^{10}, 11.3×10^{10}, and 9.3×10^{10} cm^{-2}, respectively, while the corresponding neutron SLD is 3.9×10^{10}, 1.65×10^{10}, and 6.33×10^{10} cm^{-2}. It can be seen that the neutron SLD contrast of dendrimer in D_2O is 1.93 times that of DNA, whereas the X-ray SLD contrast of DNA is 3.15 times that of dendrimer. The SANS intensity of the dendriplex should thus be dominated by the dendrimer component, in particular that the large size of G9 dendrimer prescribes a large magnitude of $S_{dd}(q)$ in the low-q region. In this case, the SANS curve may directly reflect the spatial organization of dendrimer in the complex. On the other hand, DNA may dominate the X-ray scattering intensity, such that the SAXS profile may reveal the structure features of DNA in the dendriplex.[15,16]

The charge density of PAMAM G9 dendrimer was prescribed by its dp value which stands for the number fraction of protonated amine groups in the dendrimer. The nominal N/P ratio of the dendriplex, prescribed by the feed ratio of the number of moles of amine groups (N, including both primary and tertiary amine groups) to that of phosphate groups of DNA (P), was fixed at 6/1.

dx.doi.org/10.1021/ma300308y | Macromolecules 2012, 45, 5208−5217

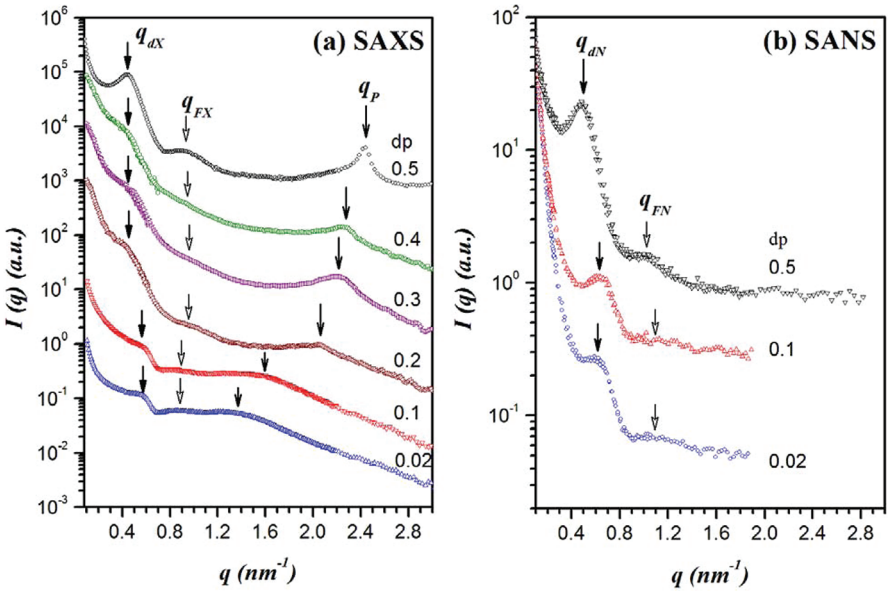

Figure 1. (a) SAXS profiles of DNA–PAMAM G9 dendrimer complex with different dendrimer dp values ranging from 0.02 to 0.5. (b) SANS profiles of the dendriplexes with three selected dp values.

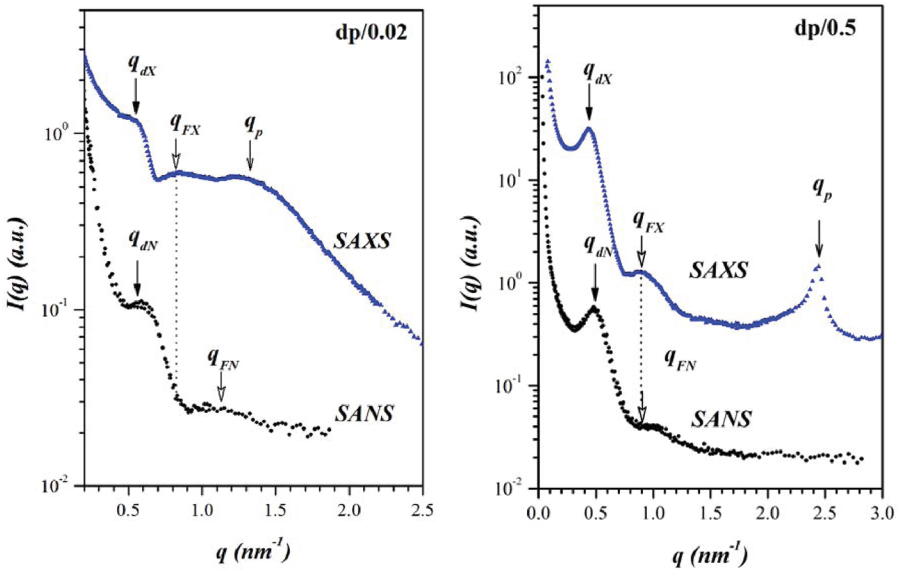

Figure 2. SAXS profiles of dp/0.02 and 0.5 dendriplexes along with the corresponding SANS profiles for clearer demonstration of the differences between these two types of scattering patterns.

Figure 1a displays the SAXS profiles, more sensitive to DNA than dendrimer, of the complexes with G9 dendrimers with different dp values ranging from 0.02 to 0.5. The profiles were vertically shifted to avoid overlaps. The scattering patterns were different from those associated with the ordered columnar mesophases found for the dendriplexes with low-generation dendrimers.[16] For dp < 0.5, the SAXS pattern was characterized by a shoulder (marked by "q_{dX}") near 0.5 nm^{-1}, a small hump (marked by "q_{FX}") at ca. 0.8 nm^{-1}, and a large broad shoulder or peak (marked by "q_p") near 1.4–2.0 nm^{-1}. When the d*p* value was increased to 0.5, the SAXS profile exhibited a sharper primary peak at q_{dX} and a clear q_{FX} peak. An additional sharp peak (q_p) was identified at 2.5 nm^{-1}.

The SANS profiles, more sensitive to dendrimer than DNA, of the dendriplexes with three selected dp values are displayed in Figure 1b. The scattering curves were seen to exhibit a primary peak (q_{dN}) near 0.5 nm^{-1} and a small shoulder (marked by "q_{FN}") beside it. The q_p peaks found in the SAXS profiles were not visible in SANS patterns; therefore, the SAXS curves showed an additional q_p peak in the high-*q* region. This feature was demonstrated more clearly in Figure 2 which plotted the SAXS profiles of dp/0.02 and 0.5 dendriplexes along with the corresponding SANS profiles. The q_p peaks observed in the SAXS profiles were absent in the SANS curves. The primary peak (i.e., q_{dX} peak) in the SAXS profile located at approximately the same position as q_{dN} peak in the corresponding SANS curve. The q_{FX} peak of dp/0.02 dendriplex however situated at lower *q* than the corresponding q_{FN} peak, but these two peaks were found to locate at approximately the same position for dp/0.5 complex. Figure 3 plots q_{dX}, q_{dN}, q_{FX}, and q_{FN} as a function of dp. It can be seen that the difference between q_{FX} and q_{FN} was significant at lower

dx.doi.org/10.1021/ma300308y | *Macromolecules* 2012, 45, 5208–5217

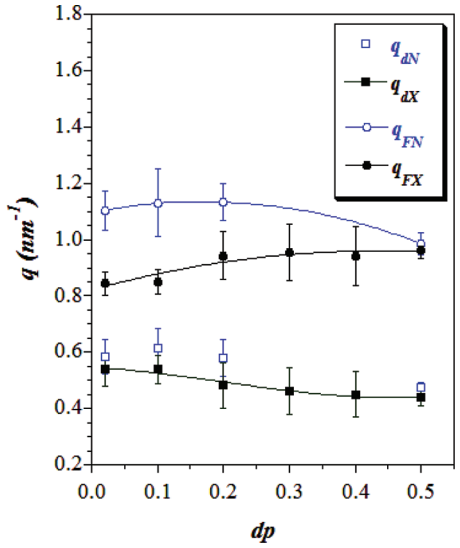

Figure 3. q_{dX}, q_{dN}, q_{FX}, and q_{FN} as a function of dp. It can be seen that the difference between q_{FX} and q_{FN} was significant at lower dp values (dp < 0.3), while they closely agreed with each other for dp/0.5 dendriplex.

dp values (dp < 0.3), while they closely agreed with each other for dp/0.5 dendriplex. The difference implied that q_{FX} and q_{FN} were of different origin, which may be due to the fact the SANS intensity was dominated by the dendrimer component, while DNA should make a significant contribution to the SAXS intensity. This will be clarified later by scattering function calculation of model structure.

Baldwin et al. have reported a series of SANS profiles of concentrated chromatin solution of DNA/histone in D_2O/H_2O mixture for contrast variation experiment.[22] In 100% D_2O the scattering profile was found to exhibit a primary peak (with the characteristic spacing D of 10.5 nm) along with a smaller shoulder at higher q. With the increase of H_2O content, the primary peak diminished in intensity and additional peaks (corresponding to D = 5.5 and 2.7 nm) emerged in the high-q region; the SANS profile collected at 10% D_2O, which showed a primary peak along with two high-q peaks, was close to their observed SAXS profile. Such a scattering pattern was indeed similar to the SAXS profiles of dp/0.02 and 0.1 dendriplexes (Figure 1a). Consequently, the present dendriplex system exhibited analogous scattering behavior to that of chromatin in terms of the feature of their SAXS profiles and the fact that SAXS curves always showed additional high-q peaks comparing to the SANS profiles. These similarities strongly suggested that DNA in the dendriplex wrapped around PAMAM G9 dendrimer to form the beads-on-string structure, as schematically illustrated in Figure 4a.

Our previous study of the complexes of DNA with PAMAM G4 dendrimer showed that beads-on-string structure was accessible when more than a half of the amine groups in the dendrimer were positively charged (i.e., each dendrimer macrocation carried more than 64 positive charges).[15] A PAMAM G9 dendrimer contains a total of 4094 amine groups; each macrocation thus carries about 82 positive charges even at dp as low as 0.02. The stronger electrostatic attraction coupled with lower bending energy cost (comparing to G4 dendriplex) may easily induce DNA to wrap around the dendrimer for effective charge matching. Since the DNA used here had 9200 base pairs with the fully extended length of ca. 3 μm, each DNA chain was able to wrap around a number of G9 dendrimer (diameter = 11.4 nm), giving rise to the "chromatin-like fiber" composing of the "nucleosome-like particles". Such a beads-on-string structure is characterized by a characteristic interparticle distance d and a pitch length P of the DNA superhelix wrapping around the dendrimer (see Figure 4a).

In the case of G4 dendriplex showing beads-on-string structure, the SAXS profile (which was dominated by DNA) displayed a small peak at lower q (q_d, equivalent to q_{dX} in this study) and a stronger peak at high q (q_P). From the calculation of the SAXS pattern of model beads-on-string structure, the q_d

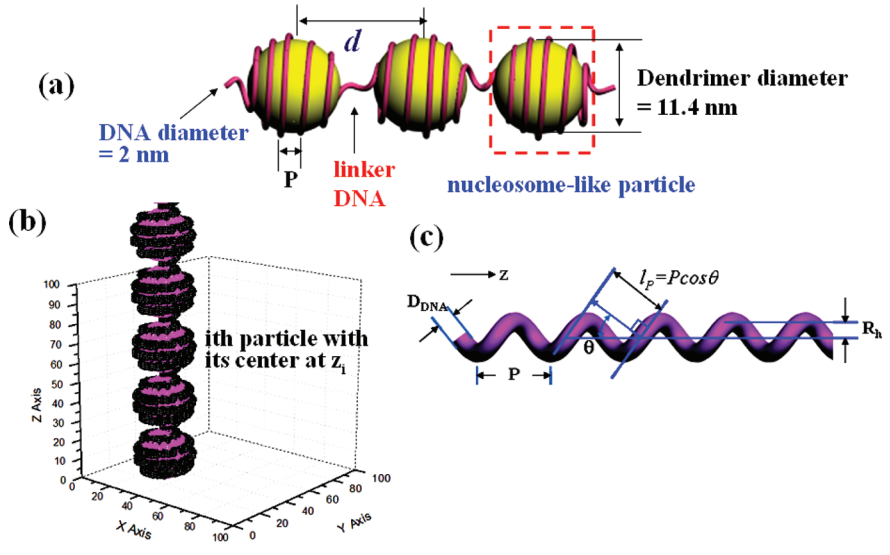

Figure 4. (a) Schematic illustration of the beads-on-string structure. This structure is characterized by a characteristic interparticle distance d and a pitch length P of the DNA superhelix wrapping around the dendrimer. (b) Real-space picture of the stiff chromatin-like fiber generated for calculating the scattering curves. (c) Definitions of the geometric parameters of a DNA superhelix used for model calculation. P and θ represent the pitch length and pitch angle, respectively. R_h is the radius of the superhelix defined as the radial distance between the centerline and central trace of the helix.

dx.doi.org/10.1021/ma300308y | Macromolecules 2012, 45, 5208−5217

peak was found to arise from the interparticle distance ($d = 2\pi/q_d$) between the nucleosome-like particles in the chromatin-like fiber which was assumed to be a stiff rod with the nucleosome-like particles arranging in a linear array, while the q_p peak was due to the pitch length of the DNA superhelix ($P = 2\pi/q_P$). On the basis of this finding, we considered the primary peak (i.e., q_{dX} and q_{dN}) at ca. 0.5 nm^{-1} in the scattering profiles of the DNA−PAMAM G9 complex to be associated with the interparticle distance of the nucleosome-like particles in the chromatin-like fiber. The shoulder or peak (i.e., q_P) appearing only in the high-q region (q = 1.3 or 2.4 nm^{-1}) of the SAXS profile was attributed to the pitch length of the DNA superhelix. The fact that the primary peak was broad and relatively weak in intensity at dp < 0.5 implied that the conformation of the chromatin-like fiber formed may deviate from stiff rod due to orientation fluctuations (which will be described in detail in section 3) of the nucleosome-like particles about the fiber axis (see Figure 5). In this case, the distribution of the "effective interparticle distance" (d_{eff}, the projected length of d onto the fiber axis) between the nucleosome-like particles along the fiber axis was broad (see Figure 5), thereby leading to broad primary peak. The primary peak became sharper and more intense when dp was increased to 0.5, implying that the chromain-like fiber became stiffer.

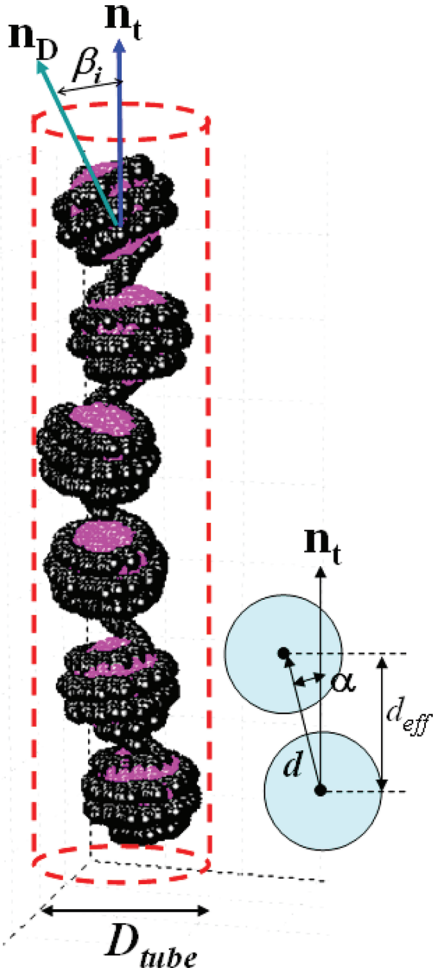

Figure 5. Schematic illustration of the wormlike chromatin-like fiber model. The orientation fluctuation of the vector **d** (connecting two neighboring particles) under a constant length |**d**| with respect to $\mathbf{n}_t$ (characterized by the angle α) and the orientation fluctuation of the superhelix axis $\mathbf{n}_D$ with respect to $\mathbf{n}_t$ (characterized by the angle β) are assumed to be independent of each other.

2. Calculation of Scattering Profiles for dp/0.5 Dendriplex Using "Stiff Chromatin-like Fiber Model". The "stiff chromatin-like fiber model" previously used to analyze the SAXS profile of G4 dendriplex[15] was adopted to calculate the scattering profiles of the dp/0.5 complex. Here we constructed a stiff rodlike fiber formed by a DNA chain and dendrimers in which the DNA chain wraps around a number of dendrimer macrocations along a fiber axis (i.e., z-axis) (Figure 4b). Each dendrimer was approximated by a sphere linked with the intersphere distance d (Figure 4a). The DNA superhelix was approximated by a uniform helical cylinder with a given pitch length P and pitch angle θ (Figure 4c).[15] The radius of the superhelix (R_h) given by $R_h = P/(2\pi \tan\theta)$ is defined as the radial distance between the centerline and central trace of the helix ($R_h = 0$ for completely straightened DNA). Therefore, the helical trace of the cylinder can be calculated from the equations[24]

$$x(z) = R_h \sin\left(\frac{2\pi z}{P} + \varphi\right); \quad y(z) = R_h \cos\left(\frac{2\pi z}{P} + \varphi\right)$$

where ϕ is the phase angle that defines the sense of the superhelix. The regular pitch of a helix can give rise to a scattering peak locating at $q_p \approx 2\pi/l_P = 2\pi/(P\cos\theta)$, where l_P is the projection of P onto the normal of the helical segment (Figure 4c). It can be shown that $q_p \approx 2\pi/l_P$ as long as $2\pi R_h$ is significantly larger than P.

The wrapping of DNA around the dendrimer was assumed to be tight with a constant pitch length; moreover, since d was normally larger than the diameter of dendrimer, a rodlike linker DNA was incorporated between two successive nucleosome-like particles.[25,26] We assumed that DNA wrapped around dendrimer i from one pole (locating at $z = z_i - R_{den} - R_{DNA}$ with R_{den} and R_{DNA} being the radius of dendrimer and DNA, respectively, and z_i being the central position of sphere i in the one-dimensional array) to another pole (locating at $z = z_i + R_{den} + R_{DNA}$). In such a nucleosome-like particle, the value of R_h associated with the helical trace of DNA continuously varied with z (see eq 2). The rodlike linker DNA (with $R_h = 0$) between sphere i and $i + 1$ was also assumed to be placed from the pole (at $z = z_i + R_{den} + R_{DNA}$) of sphere i to the pole (at $z = z_{i+1} - R_{den} - R_{DNA}$) of sphere $i + 1$ with a constant length.

$$R_h(z) = \begin{cases} \sqrt{(R_{den} + R_{DNA})^2 - (z - z_i)^2}, \\ \quad \text{for } z_i - R_{den} - R_{DNA} \\ \quad \le z \\ \quad \le z_i + R_{den} + R_{DNA} \\ 0, \quad \text{for } z_i + R_{den} + R_{DNA} \\ \quad < z \\ \quad < z_{i+1} - R_{den} - R_{DNA} \end{cases} \tag{2}$$

In the previous study of the beads-on-string structure of G4 dendriplex, we found that a portion of the body of DNA penetrated into the interior of dendrimer while wrapping around it.[15] Because the number (= 2048) of primary amine groups of G9 dendrimer is huge, the surface monomer density would have been exceedingly high, if all these amine groups were located at the periphery. Therefore, a portion of the primary amine groups should back-fold into the interior of the dendrimer,[27] such that the probability of finding the charged

dx.doi.org/10.1021/ma300308y | Macromolecules 2012, 45, 5208−5217

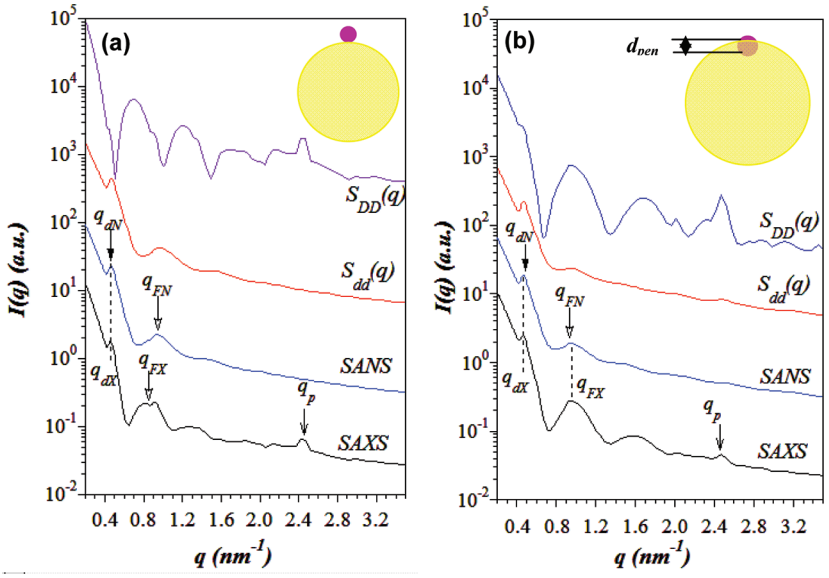

Figure 6. Calculated SAXS and SANS profiles for the stiff chromatin-like fiber composing of 10 nucleosome-like particles with P = 2.6 nm and d = 14 nm. The partial structure factors, $S_{DD}(q)$ and $S_{dd}(q)$, are also displayed. The radial penetration depth of DNA assumed is (a) d_{pen} = 0 and (b) d_{pen} = 1.5 nm.

ammonium groups at the interior increased with increasing dp value. DNA may thus penetrate into the dendrimer while wrapping around it for charge matching, especially at higher dp values. Such a penetration was also taken into account in the scattering function calculation. In this case, the body of the DNA superhelix was assumed to move into the dendrimer along the $-r$ direction (i.e., opposite to the radial direction) of the spherical macrocation by a distance of d_{pen}, as schematically illustrated in the insets of Figure 6.

After constructing the chromatin-like fiber with given values of P, d, and the radial penetration depth (d_{pen}), we divided the system into numerous volume elements (each with the size of 8 × 8 × 8 Å^3), and the partial structure factors for the randomly oriented chromatin-like fiber were calculated by the Debye equation, viz.[28]

$$S_{dd}(q) = \sum_{i\in G9}\sum_{j\in G9}\frac{\sin(q|\mathbf{r}_i - \mathbf{r}_j|)}{q|\mathbf{r}_i - \mathbf{r}_j|} \quad (3)$$

$$S_{DD}(q) = \sum_{i\in \mathrm{DNA}}\sum_{j\in \mathrm{DNA}}\frac{\sin(q|\mathbf{r}_i - \mathbf{r}_j|)}{q|\mathbf{r}_i - \mathbf{r}_j|} \quad (4)$$

$$S_{Dd}(q) = \sum_{i\in \mathrm{DNA}}\sum_{j\in G9}\frac{\sin(q|\mathbf{r}_i - \mathbf{r}_j|)}{q|\mathbf{r}_i - \mathbf{r}_j|} \quad (5)$$

where i and j belong to the dendrimers (G9) for S_{dd}, DNAs for S_{DD} and DNA and G9 for S_{Dd}, and $|\mathbf{r}_i - \mathbf{r}_j|$ is the distance between i and j volume element.[27] The SAXS and SANS intensities were then calculated from the three partial structure factors by eq 1. It should be noted that the approximation of dendrimer molecule by uniform sphere is an oversimplification since the monomers constituting the molecule undergo density fluctuations, leading to an excess intensity that causes smearing of the form factor peaks in the scattering profile.[23] Therefore, an excess intensity arising from such a density fluctuation was eventually added to the scattering intensity calculated by eq 1, such that the calculated scattering curves appeared more similar to the experimentally observed ones. It is further noted that we will not be able to obtain the scattering profiles that quantitatively predict the experimental results from the rather idealized model. Here we merely sought the structure that accounted for the qualitative features of the experimental scattering profiles and from which we could identify the salient features of the beads-on-string structures formed at different dendrimer charge densities.

Figure 6 shows the calculated SAXS and SANS profiles for the stiff chromatin-like fiber composing of 10 nucleosome-like particles with P = 2.6 nm, d = 14 nm, and R_{den} = 5.7 nm. The partial structure factors, $S_{DD}(q)$ and $S_{dd}(q)$, are also displayed. The model associated with Figure 6a assumed no penetration of DNA (d_{pen} = 0 nm), while that for Figure 6b assumed d_{pen} = 1.5 nm. The shapes of the calculated scattering curves closely resembled the observed scattering profiles of the dp/0.5 dendriplex, where there existed a relatively sharp primary peak at ca. 0.4 nm^{-1} followed by a hump near 0.8 nm^{-1}, and the calculated SAXS curve further displayed a peak at 2.4 nm^{-1}. This close similarity signals that dp/0.5 dendriplex formed the beads-on-string structure, and the resultant chromatin-like fiber was stiff. Comparison between the scattering patterns and the partial structure factors showed that the calculated SANS profiles were essentially identical to $S_{dd}(q)$ calculated for both d_{pen} = 0 and 1.5 nm, elucidating that the dendrimer dominated the neutron scattering intensity. The position of the primary peak in SANS profile (q_{dN}) was found to be determined by the interparticle distance of the dendrimer macrocations (or nucleosome-like particles) along fiber axis ($q_{dN} = 2\pi/d$). The peak q_{FN} corresponded to the first-order form factor maximum of the dendrimer.

For the SAXS profiles, $S_{dd}(q)$ still dominated the scattering profile at q < 0.6 nm^{-1}, similarly to the case of the SANS profile, such that the primary peak (q_{dX}) was also determined by the interparticle distance of the nucleosome-like particles. However, $S_{DD}(q)$ contributed significantly to the X-ray scattering intensity at higher q, and a peak (at q_P) associated with the pitch length ($P \approx 2\pi/q_p$) of the DNA superhelix wrapping around the dendrimer was observable at 2.4 nm^{-1}. The intensity of this peak depended on the number of

dx.doi.org/10.1021/ma300308y | Macromolecules 2012, 45, 5208−5217

nucleosome-like particles in the fiber assumed for the calculation under a given P; the peak dropped in intensity with decreasing number of nucleosome-like particles, which in turn caused an apparent broadening of the peak relative to the background scattering intensity $[\sim S_{dd}(q)]$ which existed underneath the peak. This is because that the drop of the peak intensity [due to $S_{DD}(q)$] is expected to be larger than the drop of the background intensity associated with $S_{dd}(q)$ with decreasing number of particles. Consequently, a stiff chromatin-like fiber with a larger number of nucleosome-like particles tends to exhibit a clearer peak at q_p along with a sharper peak at q_{dX} in the SAXS profile, although this effect was not explicitly shown in Figure 6.

The position of q_{FX} peak was found to depend on the radius of the DNA superhelix (R_h), whose value decreased with increasing DNA penetration depth. This peak shifted to a higher q value with increasing d_{pen} (q_{FX} = 0.85 and 0.98 nm^{-1} for d_{pen} = 0 and 1.5 nm, respectively). Moreover, a comparison between q_{FX} and q_{FN} in the calculated scattering profiles indicated that q_{FN} located at a higher q than q_{FX} for d_{pen} = 0. This trend of $q_{FN} > q_{FX}$ was clearly evidenced for dp $\leq$ 0.4 by the experimental results shown in Figure 3. On the other hand, q_{FX} and q_{FN} situated at approximately the same position for d_{pen} = 1.5 nm (as observed for dp/05 dendriplex in Figure 3). In light of this finding, the progressive shift of q_{FX} to higher q with increasing dp as elucidated in Figure 3 was attributed to the increasing penetration depth of DNA into the dendrimer while wrapping around it.

Figure 7 compares the calculated SAXS and SANS profiles (using d = 14 nm, P = 2.6 nm, and d_{pen} = 1.0 nm) with the observed SAXS and SANS scattering profiles to demonstrate the close resemblance of the calculated curves to the experimental data. The pitch length obtained, corresponding to the wrapping of DNA around each dendrimer macrocation by 4.4 turns, was slightly larger than the diameter of B-DNA (= 2 nm),[29] showing that the DNA segments were closely spaced along the fiber axis to effectively match the positive charges on dendrimer.

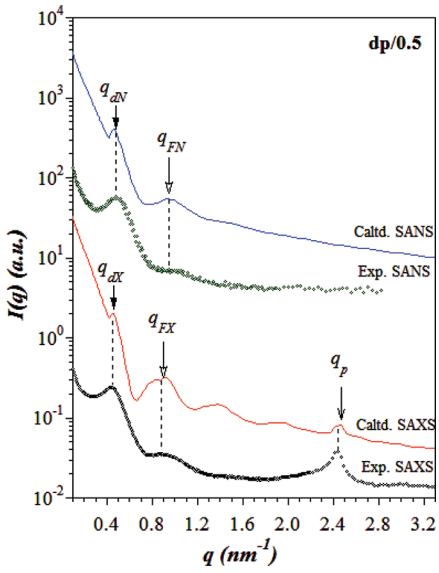

Figure 7. Comparison between the calculated SAXS and SANS profiles (using d = 14 nm, P = 2.6 nm, and d_{pen} = 1.0 nm) with the observed scattering profiles of dp/0.5 dendriplex to demonstrate the close resemblance of calculated curves to the experimental data.

3. Calculation of Scattering Profiles for Ddendriplexes with dp < 0.5 Using "Wormlike Chromatin-like Fiber Model". Based on the foregoing discussion, the chromatin-like fiber formed at dp < 0.5 should be more flexible, as evidenced by less distinct and broader scattering peaks at q_{dX}, q_{dN}, and q_P. A "wormlike chromatin-like fiber" model was hence introduced to investigate their scattering profiles. We first constructed an imaginary tube with the diameter of D_{tube} to confine the chromatin-like fiber, as shown in Figure 5. The nucleosome-like particles were then placed sequentially within the tube under the constraint of a constant value of d. The center-of-mass of each particle was placed under the constraint that it retained the constant distance of d from its predecessor. A wormlike chromatin-like fiber was then generated after placing a prescribed number of nucleosome-like particles in the tube. Thus, the vector $\mathbf{d}$ connecting neighboring centers of the particles has some orientation fluctuations with respect to $\mathbf{n}_t$ as specified by the angle $\boldsymbol{\alpha}$ between $\mathbf{d}$ and $\mathbf{n}_t$, where $\mathbf{n}_t$ is the unit vector parallel to the tube axis (Figure 5). In general, the larger the chosen value of D_{tube}, the more flexible the fiber appeared. In addition to the orientation fluctuations of the vector $\mathbf{d}$ within the tube, we also allowed the orientation fluctuations of the particles caused by the DNA wrapping, which were characterized by the angle β between the tube axis ($\mathbf{n}_t$) and the DNA superhelix axis defined by the unit vector $\mathbf{n}_D$ (Figure 5). In this case, we set a maximum difference between β of the particle and that of its predecessor, $\Delta\beta_{max}$. Then, the value of β of particle i + 1 was given by $\beta_{i+1} = \beta_i + \Delta\beta$ with the value of $\Delta\beta$ chosen randomly between $-\Delta\beta_{max}$ and $\Delta\beta_{max}$. We assumed that the two orientation fluctuations of $\mathbf{d}$ and $\mathbf{n}_D$ as specified by the angles α and β, respectively, are independent of each other. The chromatin-like fiber generated each time within the tube only represented a snapshot of the constantly fluctuating conformation of the fiber; therefore, the formal scattering curve of the wormlike fiber was obtained by averaging the scattering intensity profiles of about 10 such snapshots.

Figure 8a compares the SAXS profile of dp/0.02 dendriplex with the scattering curve calculated using the parameters listed in Table 1. The DNA penetration depth d_{pen} was set as zero in the calculation. It can be seen that the model adopted produced the SAXS profile resembling the observed ones. The broad shoulder near 1.3 nm^{-1} was found to correspond to the pitch peak of the DNA superhelix. Our model calculation actually revealed that the orientation fluctuations of the vector $\mathbf{d}$ caused broadening or shoulder-like shape of the primary peak, while the orientation fluctuations of the DNA superhelix axes with respect to β exerted the same effect on the pitch peak, although the latter effect is not explicitly shown in Figure 8. The comparisons between the observed and calculated SAXS profiles for the dendriplexes with another two dp values are shown in Figure 8b.

4. Self-Assembling Mechanism of Chromatin-like Fiber and Physical Factors Controlling the Fiber Structure. It may be important to consider a balance of various forces acting in the system in order to visualize a plausible self-assembling mechanism of the chromatin-like fiber structure of the dendriplex: (1) electrostatic attractive force f_{dD} between the positively charged dendrimers and the negatively charged DNA,[30] (2) electrostatic repulsive force f_{DD} between DNA and DNA or f_{dd} between dendrimers and dendrimers, (3) repulsive forces f_{ex} due to excluded volume effects among

dx.doi.org/10.1021/ma300308y | Macromolecules 2012, 45, 5208−5217

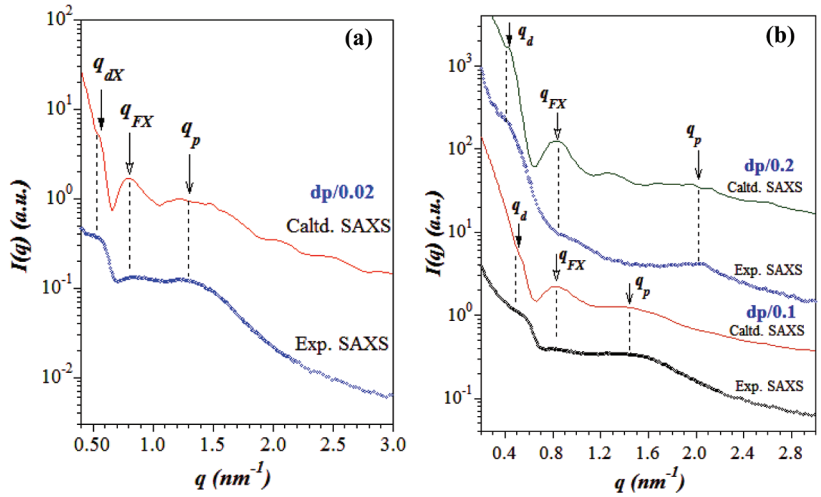

Figure 8. Comparison between the observed SAXS profiles of (a) dp/0.02 and (b) dp/0.1 and 0.2 dendriplexes and the SAXS curves calculated using wormlike chromatin-like fiber model.

Table 1. Values of the Parameters Used for Calculating the Scattering Profiles by Wormlike Chromatin-like Fiber Model

dp	d (nm)	P (nm)	D_{tube} (nm)	$\Delta\beta_{max}$
0.02	11.6	4.50	20.0	50
0.10	11.7	4.00	20.0	50
0.20	13.0	3.00	20.0	50
0.30	13.6	2.85	20.0	50
0.40	13.9	2.80	20.0	50
0.50	14.0	2.60		

dendrimers−dendrimers, dendrimers−DNAs, and DNAs−DNAs, and (4) random thermal force f_{ran} which maximizes translational entropy of dendrimers and DNAs.

The attractive force f_{dD} outweighs the "entropic force" f_{ran}, so that the dendrimers are enriched along the wormlike DNA chains with average interdendrimer distances being separated sufficiently apart to reduce the repulsive forces f_{dd}. Let us define this hypothetical situation as a "loose wormlike dendriplex", as illustrated in Figure 9a. Whether the loose wormlike dendriplexes (part a) grow into the chromatin-like fiber having the beads-on-string structures (from part b1 to b2) or the columnar mesophase (part c2) via a lateral packing of the loose wormlike dendriplexes (part c1) depends on the balance of (5) the bending force of DNA f_{bend} against the attractive force f_{dD}. As already pointed out, the PAMAM G9 dendrimer satisfies the criterion of $f_{dD} > f_{bend}$, while the lower-generation PAMAM dendrimers satisfy the criterion of $f_{dD} < f_{bend}$. In order to verify the crude model for the self-assembling process and mechanism discussed above (part a to b1 and b2 or to c1 and c2), it is crucial to conduct time-resolved SAXS and SANS experiments, which definitely deserves future works.

The pitch length and the interparticle distance associated with the beads-on-string structure deduced from the scattering profile calculation are plotted as a function of dp in Figure 10. The interparticle distance d was seen to increase with increasing dp, presumably due to the stronger electrostatic repulsive force f_{DD} between the nucleosome-like particles at higher dp as a result of the presence of more unmatched ammonium groups (such that the nucleosome-like particles were overcharged). The pitch length P decreased abruptly with increasing dp in the small dp range of dp < 0.2, but the tendency became weaker at higher dp. The smaller pitch length observed at higher dp is

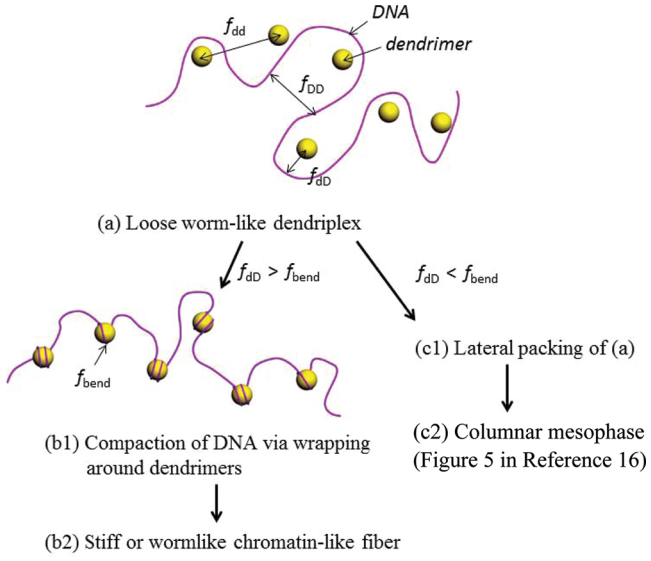

Figure 9. Possible self-assembling mechanism of the dendriplexes (a) into stiff or wormlike chromatin-like fiber (b2) through the compaction of DNA via wrapping around dendrimers (b1) or into the columnar mesophase (c2) through a process (c1) of the lateral packing of (a).

attributable to the tendency to enhance the charge matching; however, enhancement of charge matching would cost the bending energy of DNA and the balance between electrostatic interaction energy and bending energy (i.e., $f_{dD} > f_{bend}$) may lead to the observed variation of pitch length with dp.

It should be noted that while the present calculation was able to reveal the salient feature of the beads-on-string structure formed by the dendriplex, the persistence length of the chromatin-like fiber could not be quantitatively determined experimentally, because the q-range covered in this experiment was not small enough. The experimental determination requires $I(q)$ in the q-range much smaller than the q_{dN} or q_{dX}. Nevertheless, the fact that both the primary peak and the pitch peak clearly sharpened when dp was increased from 0.4 to 0.5 indicated that the chromatin-like fiber underwent a stiffening across this change of dp. The large stiffness may stem from the strong electrostatic repulsion between the overcharged

dx.doi.org/10.1021/ma300308y | Macromolecules 2012, 45, 5208−5217

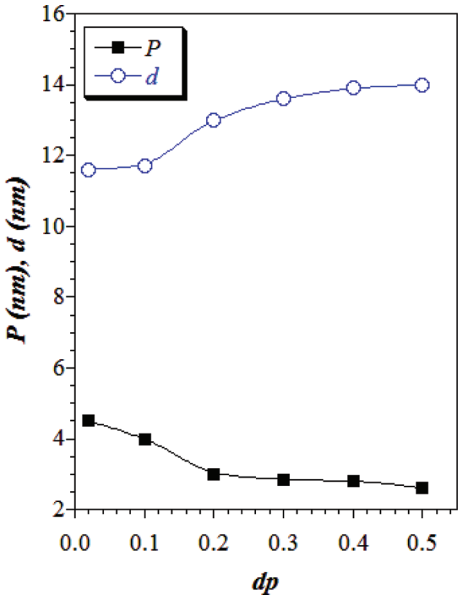

Figure 10. Pitch length and the interparticle distance associated with the beads-on-string structure deduced from the scattering profile calculation as a function of dendrimer dp value.

nucleosome-like particles. The abrupt conformational flexibility change with respect to the increase of dp seems to be common to the cooperative phenomenon and phase transition observed in various one-dimensional systems. Profound theoretical studies may be necessary to gain detailed insight into this phenomenon.

CONCLUSIONS

We have shown that DNA was able to wrap around PAMAM G9 dendrimer to form beads-on-string structure even at very low dendrimer charge density. In this sense, PAMAM dendrimers of high generations may serve as a plausible model system with tunable charge densities for facilitating the understanding of DNA–histone complexation. The present study also demonstrated the power of SAXS and SANS in resolving the structure details (including the pitch length of the DNA superhelix wrapping around the dendrimer, the interparticle distance of the nucleosome-like particles constituting the chromatin-like fiber, and even the conformational flexibility of the fiber) based on the calculation of scattering patterns of appropriate model structures. The interparticle distance of the nucleosome-like particles and the pitch length of the DNA superhelix were found to increase and decrease with increasing dendrimer dp, respectively. At lower dendrimer charge densities (i.e., dp $\leq$ 0.4), the chromatin-like fibers formed by the dendriplex exhibited conformational flexibility with orientation fluctuations of the nucleosome-like particles. When dendrimer dp was increased to 0.5, the chromatin-like fiber became stiff, leading to sharp interparticle correlation peak and pitch peak in the SAXS profile.

AUTHOR INFORMATION

Corresponding Author

*E-mail: hlchen@che.nthu.edu.tw (H.-L.C.); su.cj@nsrrc.org.tw (C.-J.S.).

Notes

The authors declare no competing financial interest.

[⊥]Professor Emeritus, Kyoto University, Kyoto 606-8501, Japan.

ACKNOWLEDGMENTS

We acknowledge the financial support of the National Science Council (NSC), Taiwan, under Grant NSC 100-2923-E-007-003. We also thank the Neutron User Program of the NSC for providing the financial support for carrying out the SANS experiments.

REFERENCES

(1) Wasylyk, B.; Chambon, P. *Eur. J. Biochem.* **1979**, *98*, 317–327.
(2) Felsenfeld, G. *Nature* **1992**, *355*, 219–224.
(3) Bednar, J.; Horowitz, R. A.; Grigoryev, S. A.; Carruthers, L. M.; Hansen, J. C.; Koster, A. J.; Woodcock, C. L. *Proc. Natl. Acad. Sci. U. S. A.* **1998**, *95*, 14173–14178.
(4) Netz, R. R.; Joanny, J.-F. *Macromolecules* **1999**, *32*, 9026–9040.
(5) Jonsson, M.; Linse, P. *J. Chem. Phys.* **2001**, *115*, 10975–10985.
(6) Kunze, K. K.; Netz, R. R. *Phys. Rev. Lett.* **2000**, *85*, 4389–4392.
(7) Kunze, K. K.; Netz, R. R. *Phys. Rev. E: Stat., Nonlinear, Soft Matter Phys.* **2002**, *66*, 011918.
(8) Zinchenko, A. A.; Luckel, F.; Yoshikawa, K. *Biophys. J.* **2007**, *92*, 1318–1325.
(9) Zinchenko, A. A.; Yoshikawa, K.; Baigl, D. *Phys. Rev. Lett.* **2005**, *95*, 228101.
(10) Tomaila, D. A.; Baker, H.; Dewald, J.; Hall, M.; Kallos, G.; Martin, S.; Roeck, J.; Ryder, J.; Smith, P. *Polym. J.* **1985**, *17*, 117–132.
(11) Esfand, R.; Tomaila, D. A. *Drug Discovery Today* **2001**, *6*, 427–436.
(12) Ottaviani, M. F.; Sacchi, B.; Turro, N. J.; Chen, W.; Jockusch, S.; Tomalia, D. A. *Macromolecules* **1999**, *32*, 2275–2282.
(13) Brothers, H. M., II; Piehler, L. T.; Tomalia, D. A. *J. Chromatogr.* **1998**, *A814*, 233–246.
(14) Bielinska, A. U.; Chen, C. L.; Johnson, J.; Baker, J. R. *Bioconjugate Chem.* **1999**, *10*, 843–850.
(15) Chen, C. Y.; Su, C. J.; Peng, S. F.; Chen, H. L.; Sung, H. W. *Soft Matter* **2011**, *7*, 61–63.
(16) Su, C. J.; Chen, H. L.; Wei, M. C.; Peng, S. F.; Sung, H. W.; Ivanov, V. A. *Biomacromolecules* **2009**, *10*, 773–783.
(17) Liu, Y. C.; Chen, H. L.; Su, C. J.; Liu, H. K.; Liu, W. L.; Jeng, U. *Macromolecules* **2005**, *38*, 9434–9440.
(18) Evans, H. M.; Ahmad, A.; Ewert, K.; Pfohl, T.; Martin-Herranz, A.; Bruinsma, R. F.; Safinya, C. R. *Phys. Rev. Lett.* **2003**, *91* (7), 075501–1.
(19) Dootz, R.; Toma, A. C.; Pfohl, T. *Soft Matter* **2011**, *7*, 8343–8351.
(20) Ottaviani, M. F.; Furini, F.; Casini, A.; Turro, N. J.; Jockusch, S.; Tomalia, D. A.; Messori, L. *Macromolecules* **2000**, *33*, 7842–7851.
(21) Cakara, D.; Kleimann, J.; Borkovec, M. *Macromolecules* **2003**, *36*, 4201–4207.
(22) Baldwin, J. P.; Boseley, P. G.; Bradbury, E. M.; Ibel, K. *Nature* **1975**, *253*, 245–249.
(23) Porcar, L.; Liu, Y.; Verduzco, R.; Hong, K.; Butker, P. D.; Magid, L. J.; Smith, G. S.; Chen, W. R. *J. Phys. Chem. B* **2008**, *112*, 14772–14778.
(24) Hamley, I. W. *Macromolecules* **2008**, *41*, 8948–8950.
(25) Larin, S. V.; Darinskii, A. A.; Lyulin, A. V.; Lyulin, S. V. *J. Phys. Chem. B* **2010**, *114*, 2910–2919.
(26) Qamhieh, K.; Nylander, T.; Ainalem, M.-L. *Biomacromolecules* **2009**, *10*, 1720–1726.
(27) Porcar, L.; Hong, K.; Butler, P. D.; Herwig, K. W.; Smith, G. S.; Liu, Y.; Chen, W. R. *J. Phys. Chem. B* **2010**, *114*, 1751–1756.
(28) Debye, P. *Ann. Phys.* **1915**, *46*, 809.
(29) Müller, J. J. *J. Appl. Crystallogr.* **1983**, *16*, 74–82.
(30) f_{dD} is composed of two contributions. The first arises from the direct electrostatic attraction between the negatively charged phosphate group and positively charged ammonium group. The other stems from the entropic gain associated with the release of the originally condensed counterions Na^+ and Cl^- from DNA and dendrimer, respectively, which would cause the ammonium group (or

phosphate group) to replace the originally condensed Na^+ (or Cl^-), so as to bind with the phosphate group (or ammonium group).

dx.doi.org/10.1021/ma300308y | *Macromolecules* 2012, 45, 5208−5217